

A Modified Approach for in Situ Chemical Oxidation Coupled to Biodegradation Enhances Light Nonaqueous Phase Liquid Source-Zone Remediation

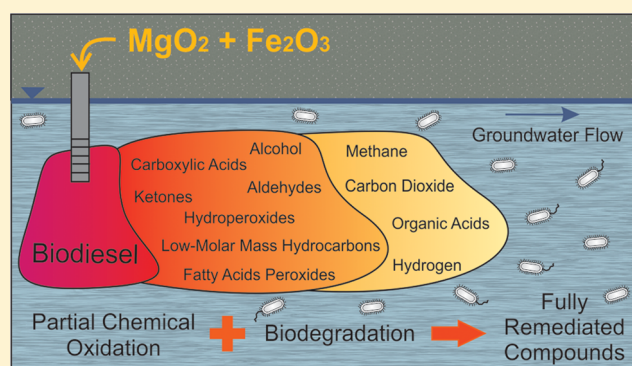
Franciele Fedrizzi,[†] Débora T. Ramos,[†] Helen S. C. Lazzarin,[†] Marilda Fernandes,[†] Catherine Larose,[‡] Timothy M. Vogel,[‡] and Henry X. Corseuil^{*,†}

[†]Department of Sanitary and Environmental Engineering, Federal University of Santa Catarina, Florianópolis, Santa Catarina, Brazil

[‡]Environmental Microbial Genomics, Laboratoire Ampere, CNRS, École Centrale de Lyon, Université de Lyon, Ecully, France

Supporting Information

ABSTRACT: Field and batch experiments were conducted to assess whether a modified approach for in situ chemical oxidation (ISCO) (with MgO_2 and Fe_2O_3 particles recovered from acid mine drainage treatment) can enhance LNAPL (light nonaqueous phase liquid) dissolution and produce bioavailable soluble compounds. This modified ISCO approach was coupled to biodegradation to further remove residual compounds by microbially mediated processes. Pure palm biodiesel (B100) was chosen to represent a poorly water-soluble compound that behaves like LNAPLs, and 100 L was released to a 2 m² area excavated down to the water table. A past adjacent B100-field experiment under natural attenuation was conducted as a baseline control. Results demonstrated the enhancement of organic compound dissolution and production of soluble compounds due to the modified in situ chemical oxidation. The slow release of H_2O_2 by MgO_2 decomposition (termed partial chemical oxidation) and production of soluble compounds allowed the stimulation of microbial growth and promoted a beneficial response in microbial communities involved in oxidized biodiesel compound biodegradation. This is the first field experiment to demonstrate that this modified ISCO approach coupled to biodegradation could be a feasible strategy for the removal of poorly water-soluble compounds (e.g., biodiesel) and prevent the long-term effects generally posed in source zones.



1. INTRODUCTION

Soil and groundwater contamination by organic compounds is a widespread problem, and in situ chemical oxidation (ISCO) involving the introduction of chemical oxidants into the subsurface to transform contaminants into less harmful compounds has become a widely used technology for remediation of environments contaminated with organic compounds.^{1–3} Potassium and sodium permanganate, sodium persulfate, ozone, and Fenton's reagent [hydrogen peroxide (H_2O_2) combined with soluble iron salts] are generally used as chemical oxidants.^{1,4} Although ISCO approaches with H_2O_2 are commonly applied for organic contaminant remediation, they present technical limitations, such as ecological damage, inhibition of microbial activity,^{5–8} and rapid oxidant consumption,^{1,3} especially in groundwater contaminated with poorly water-soluble compounds where the continuous NAPL dissolution can deplete the oxidant and lead to insufficient contaminant removal.⁹ These limitations make ISCO applications with classical Fenton reactions difficult to control and predict, particularly in real environments, thus underscoring the need for field investigations that apply less aggressive and more

effective ISCO approaches to remediate poorly water-soluble compounds.

Modifications of classical Fenton reaction can be applied as alternatives to minimize technical limitations. Magnesium peroxide (MgO_2) is generally used as an oxygen release compound (ORC) in aerobic biodegradation processes.^{10–12} However, it could be potentially applied as a less aggressive approach for ISCO treatment, because it is a moderate oxidant¹¹ that allows the slow release of H_2O_2 ^{11,13–17} because of its relatively low solubility (86 mg L⁻¹)^{15,18,19} and, thus, negligibly inhibits microbial activity.¹¹ The Fenton reaction involves the decomposition of H_2O_2 catalyzed by Fe^{2+} to form the hydroxyl radical ($\cdot\text{OH}$).²⁰ Either Fe^{2+} or Fe^{3+} can be used as a catalyst for ISCO applications,²¹ but Fe^{3+} generally dominates in acidic environments due to its higher solubility under such conditions.²² The use of Fe_2O_3 particles recovered from acid mine drainage treatment (Fe_2O_3 AMD) as catalysts

Received: July 18, 2016

Revised: October 10, 2016

Accepted: November 22, 2016

Published: November 22, 2016

for the oxidation reaction was previously studied,²³ and results demonstrated an efficient catalysis of H₂O₂ that indicated that Fe₂O₃ AMD could be a low-cost and sustainable alternative to reagent-grade chemicals in the production of goethite, ferrihydrite, or magnetite (naturally occurring aquifer minerals that can catalyze H₂O₂ decomposition). Theoretically, the initiation reactions would be proceeded by MgO₂ decomposition to H₂O₂, and Fe₂O₃ dissolution to ferric iron species. Fe³⁺ would react with H₂O₂, yielding perhydroxyl, hydroperoxides, oxygen, and hydroxyl radicals, while iron cycles back and forth between Fe³⁺ and Fe²⁺ species. The initiation equations are provided in Table S1 (eqs 1–7). Therefore, the use of MgO₂ and Fe₂O₃ AMD (termed partial chemical oxidation) could be a suitable modification of the Fenton reaction and a novel approach for ISCO treatment.

When poorly water-soluble organic compounds are introduced into groundwater, they behave as nonaqueous phase liquids (NAPLs) and can exert long-term effects in contaminated sites because of their slow mass transfer and persistent NAPL dissolution to the aqueous phase. Although ISCO is generally applied for dissolved phase treatment, it can provide mass removal of contaminants in the free phase^{1,2,24} through the nonselective chemical oxidation that can break down the complexes between soil organic matter and contaminants, stripping the adsorbed contaminant from soil^{9,25} and facilitating dissolution in water. The applicability for NAPL remediation is challenging^{1,2} because ISCO alone cannot completely deplete organic compounds^{24,26} because of the contaminant rebound phenomenon, typically observed for poorly water-soluble compounds that continue to redissolve in groundwater and are conducive to oxidant depletion.^{2,3,27} However, the concurrent use of microbially mediated degradation as a biopolishing step could remove residual contaminants and allow groundwater geochemistry and ecosystem recovery.^{6,11,18,24,26,28–32} Therefore, partial chemical oxidation coupled to biodegradation (PCO-B) can enhance poorly water-soluble compound remediation by increasing the bioavailability of the parent compound³⁰ through the production of bioavailable and biodegradable oxidized metabolites³³ that could then be further removed by microbial processes.^{5,30}

In this study, pure palm biodiesel (B100) was chosen as substrate to represent LNAPL contamination due to its growing use in the worldwide energy matrix and frequent introduction into the environment through accidental or incidental spills.^{34,35} Biodiesel is mainly composed of fatty acid methyl esters (FAMES) that can be oxidized by the abstraction of a hydrogen atom from a carbon adjacent to the double bond and produce hydroperoxides. When fatty acid peroxides are formed following a complex series of reactions, they decompose into alcohols, low-molar mass hydrocarbons, ketones, and aldehydes that are then further converted to carboxylic acids, such as acetic and propionic acids^{36–39} that exhibit relatively high water solubility^{40,41} and are easily biodegradable. Thus, an enhanced dissolution of FAMES into groundwater and their subsequent conversion to more soluble and biodegradable compounds could accelerate biodiesel LNAPL remediation in subsurface environments. The termination equations are provided in Table S1 (eqs 8–11).

This study was performed with both batch and field experiments to assess the potential of partial chemical oxidation (with MgO₂ and Fe₂O₃ AMD) coupled to biodegradation (PCO-B) to enhance LNAPL source-zone remediation in

groundwater. A past adjacent B100-field experiment under monitored natural attenuation (MNA) was conducted as a baseline control.

2. MATERIALS AND METHODS

2.1. Batch Experiment. Batch experiments were conducted to determine whether partial chemical oxidation could generate H₂O₂ from MgO₂ decomposition and whether soluble compounds from palm oil oxidation are produced. These experiments were performed in sterile 100 mL glass flasks sealed with Teflon-coated septa and aluminum crimp caps, amended with 5 g of palm oil. Distilled water was added until the final volume reached 100 mL. Different sets of flasks were prepared: set 1, distilled water and Fe₂O₃; set 2, distilled water, palm oil, and Fe₂O₃; set 3, distilled water and palm oil; set 4, distilled water and MgO₂; set 5, distilled water, palm oil, and MgO₂; set 6, distilled water, palm oil, MgO₂, and Fe₂O₃. Flasks were incubated at room temperature (25 °C) for 17 days. H₂O₂ analysis was performed using a HACH 2291700 model HYP-1 hydrogen peroxide test kit (detection range of 0.2–10 mg L⁻¹). Organic compounds were analyzed and identified using an Agilent Technologies 6850 Network GC System with a 5975C VL mass spectrometer equipped with a DB-5 column (30 m × 0.25 mm × 0.10 μm). Samples were collected using a 2 mL pipet, and a liquid–liquid extraction was conducted with hexane before organic compound detection, identification, and semiquantification (based on selective ion peak surface areas). The inlet temperature was 250 °C, and the temperature program for the oven went from 50 to 300 °C at a rate of 2 °C/min.

2.2. Field Experiment. A field experiment was conducted at the Ressacada Experimental Farm in Florianópolis, SC, Brazil (latitude 27°68'S, longitude 48°53'W); 100 L of palm biodiesel (B100) was released into a 2 m² area that was excavated 1.8 m down to the water table. Iron oxide particles recovered from the AMD treatment [8.8 kg, ≈80% of active phase (Fe₂O₃)] obtained through a sequential precipitation method^{23,42} and magnesium peroxide [88 kg, ≈15% of active phase (MgO₂)] were added to promote partial chemical oxidation reaction. Because biodiesel behaves as a fixed and long-lived source with a relatively small region of influence,⁴³ its persistence and low mobility explain our focus on the source zone. Thus, the site was monitored through multilevel [depths of 2, 3, 4, 5, and 6 m below ground surface (bgs)] sampling wells (SW): SWS (source) and SW8 represented the source zone, and SW30 was used as a background well (Figure S1). Detailed information about the adjacent 100 L-field release of soybean biodiesel (B100), which was conducted as a baseline control under monitored natural attenuation conditions, is available in Figure S2. The site is mesothermic humid with an average precipitation of 1800 mm in 2014–2015, and the average groundwater temperature is 26 °C in the summer and 22 °C in the winter. Regional geology is characterized by deposits of aeolian, alluvial, lacustrine, and marine sands,⁴⁴ with 85.5% fine sand, <5% silt, and 5.5% clay. Soil organic carbon ranges between 0.06 and 1.4%. The average soil pH is 5. The groundwater flow velocity is 6 m year⁻¹, and the porosity is 0.28.

2.2.1. Groundwater Analyses. Groundwater samples were collected in capped sterile glass vials without headspace using a peristaltic pump and Teflon tubing. Groundwater samples were analyzed for acetate, propionic acid, methane, acidity, ferrous iron (Fe²⁺), redox potential, pH, dissolved oxygen, and

temperature. Acetate was analyzed by ion chromatography using a Dionex ICS-3000 instrument equipped with a conductivity detector and an AS19 column. Propionic acid measurements were taken by gas chromatography using an Agilent Technologies GC model 6890N instrument equipped with a flame ionization detector (FID), a polyethylene glycol HP-Innowax capillary column (30 m × 0.32 mm × 0.25 μm), and a model 7683 autosampler. Methane was analyzed by gas chromatography using an Agilent Technologies GC model 7890B instrument equipped with a FID, a HP 1 capillary column (30 m × 0.53 mm × 2.65 μm), and a model 7697A headspace autosampler. Acidity was analyzed by titration with the 2310B method.⁴⁵ Ferrous iron was analyzed using a HACH DR/2500 spectrophotometer, with the 1,10-phenanthroline method.⁴⁵ Redox potential, pH, dissolved oxygen, and temperature were measured on site using a QED Micropurge Flow Cell (MP20). Total organic carbon (TOC) analyses were conducted at the end of the monitoring period in the source zone of both PCO-B (after 30.6 months) and MNA (after 99.2 months) experiments to evaluate the presence of residual organic carbon in groundwater. TOC samples were analyzed by the combustion catalytic oxidation method using a TOC-V_{CPH} analyzer (Shimadzu). Detection limits were 0.1 mg L⁻¹ for acetate and propionic acid, 10 μg L⁻¹ for methane, 1 mg L⁻¹ for acidity, 0.01 mg L⁻¹ for ferrous iron, 0.2 mg L⁻¹ for dissolved oxygen, and 4 μg L⁻¹ for TOC.

2.2.2. Soil Analyses. Soil samples were collected at the end of the monitoring period for both PCO-B (after 30.6 months) and MNA (after 99.2 months) experiments to evaluate LNAPL source-zone removal. For each experiment, a hand-auger was driven into five different points distributed in the source zone and into one point in the background wells (SW30 – PCO-B and SW31 – MNA) to collect 1 kg of soil samples approximately 2 m below the ground surface (0.5 m thick soil layers). Samples were analyzed for oil and grease by the Soxhlet and silica gel extraction methods (5520D and 5520F),⁴⁵ and total organic carbon (TOC) was analyzed by the combustion catalytic oxidation method using a Nanocolor UV-vis spectrophotometer (Macherey-Nagel). The detection limit for oil and grease was 10 mg (kg of soil)⁻¹ and for TOC 5 mg (kg of soil)⁻¹. Samples were stored in plastic bags for subsequent preparation and analyses.

2.2.3. Microbial Analysis. Real-time quantitative polymerase chain reaction (qPCR) was conducted to evaluate changes in biomass (total bacteria) using the primers described in Table S2. Groundwater samples were filtered using 0.22 μm pore size Millipore membranes [poly(ether sulfone), hydrophilic]. Filters were weighed before and after groundwater sample filtration, and results are expressed in gene copies per gram of total suspended solids, as the majority of bacteria in aquifers are mainly bound to solid surfaces rather than suspended in water.^{46,47} DNA was extracted using the MoBio (Carlsbad, CA) Power Soil TM kit according to the manufacturer's protocol. The PCR mixtures for total bacteria contained 400 nM forward and reverse primers, 1× 2xSensiFAST SYBR No Rox Mix, and sterile DNAase-free water in a final volume of 20 μL. qPCR was performed using a Rotor-Gene Q (QIAGEN) thermocycler with the following temperature conditions: 95 °C for 3 min, followed by 30 cycles at 95 °C for 5 s, 60 °C for 10 s, and 72 °C for 15 s. The detection limit for the total bacterial analysis was 10² gene copies g⁻¹.

16S rRNA gene (*rrs*) sequencing was performed to assess microbial communities from both PCO-B (SWS, SW8, and

SW30) and MNA (SWS and SW31) experiments. The variable regions, V3 and V4, of the gene that encode the 16S rRNA were amplified by PCR, and sequencing was performed using Illumina MiSeq technology.⁴⁸ The first PCR cleanup was conducted with a Biometra Tpersonal ThermalCycler. Primer sequence details are given in Table S2. The PCR mixtures contained 1.5 μL of genomic DNA, 0.5 μL of amplicon PCR forward and reverse primers (10 μM), 2.5 μL of Taq Buffer 10×, 0.5 μL of Invitrogen dNTP (10 mM), 0.5 μL of Titanium Taq 50×, and 19 μL of sterile water. The final volume was 25 μL. The following cycling conditions were used for the amplification of DNA: initial denaturation at 95 °C for 3 min and 30 cycles of denaturation at 95 °C for 30 s, annealing at 55 °C for 30 s and extension at 72 °C for 30 s, followed by a final extension at 72 °C for 5 min and a hold at 10 °C. PCR products were purified using a 1.5% agarose gel with the GE Healthcare Kit [eluted with 20 μL of 10 mM Tris-HCl (pH 8.5)]. PCR-purified products were quantified using the QuantiT dsDNA HS assay kit and Qubit fluorometer (Invitrogen). The following steps were performed: second PCR cleanup, library quantification and normalization, library denaturing, and MiSeq sample loading.

Illumina reads were processed using fastx trimmer to remove barcodes (20 bp).⁴⁹ PANDAseq with a quality threshold of 0.6 was used to assemble paired-end Illumina reads,⁵⁰ and raw sequencing data were processed and analyzed using QIIME⁵¹ version 1.8.1. Quality-filtered sequences were subsequently clustered into operational taxonomic units (OTUs) at a cutoff of 97% sequence identity using the QIIME pick_closed_reference_otus.py script and the uclust algorithm.⁵² Taxonomic information for representative sequences for each OTU was gathered with the Greengenes 13 database.

2.3. Data Deposition. DNA sequences collected in this study have been deposited in NCBI (Accession Nos. PRJNA350529).

3. RESULTS AND DISCUSSION

The moderate oxidant MgO₂ was used to slowly release H₂O₂ and enhance biodiesel LNAPL dissolution in groundwater. The production of H₂O₂ by MgO₂ decomposition was demonstrated (Figure 1), and higher concentrations of H₂O₂ were detected in the flasks amended with both MgO₂ and palm oil (sets 5 and 6). This can be attributed to the presence of hydroperoxides that are commonly produced by fatty acid oxidation with H₂O₂ [Table S1 (eqs 8–11)]. Additionally, the presence of the catalyst (Fe₂O₃) enhances hydroperoxide production, which is likely to contribute to the increase in H₂O₂ concentration observed at 11 days (set 6). Furthermore, the enhanced production of reactive species by H₂O₂ decomposition might have increased the conversion of palm oil esters to low-molar mass hydrocarbons (such as alcohols, aldehydes, and ketones) as reflected by the decrease in the concentration of H₂O₂ after 17 days. In the other flasks (sets 1–4), the H₂O₂ concentration remained below 7 mg L⁻¹ and exhibited negligible variations over the 17 day incubation. The slow release of H₂O₂ is supported by the relatively high concentrations detected after 11 days as compared to those found with other ISCO approaches [i.e., CaO_{2(s)} and H₂O_{2(aq)}] in which H₂O₂ was decomposed within several hours.^{22,53,54} Thus, the slow release of H₂O₂ through MgO₂ decomposition makes it a suitable and less aggressive approach for ISCO remediation.

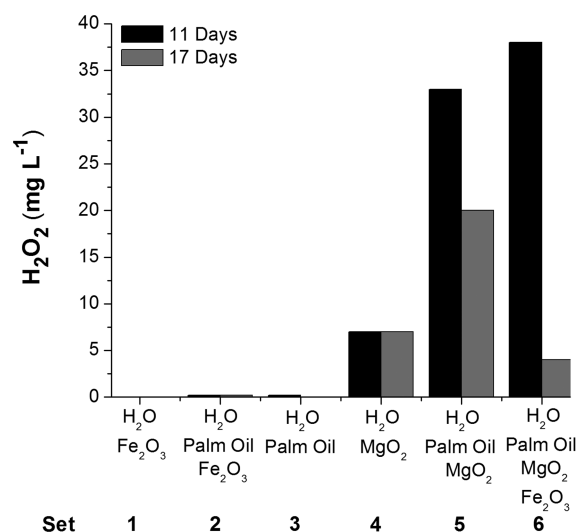


Figure 1. H₂O₂ production in different flask sets (data represent duplicate analysis). Batch experiment sets: 1, distilled water and Fe₂O₃; 2, distilled water, palm oil, and Fe₂O₃; 3, distilled water and palm oil; 4, distilled water and MgO₂; 5, distilled water, palm oil, and MgO₂; 6, distilled water, palm oil, MgO₂, and Fe₂O₃.

Poorly water-soluble organic compound remediation is often faced with limitations related to the slow dissolution to the aqueous phase and relatively low bioavailability^{5,55–57} that can be offset by the partial chemical oxidation that enhances fatty acid oxidation and dissolution leading to the production of bioavailable soluble metabolites.^{5,30} Hence, the number of soluble compounds released to the aqueous phase was significantly higher in the flask amended with MgO₂ and Fe₂O₃ than in the control in both 11 and 17 days after the start of the reaction (Figure 2A–D). Moreover, compounds closely associated with fatty acid methyl ester oxidation (such as aldehydes, alcohols, and fatty acids) were detected after 11 days (Figure 2C), whereas fewer oxidation products were observed in the control flasks. A similar pattern was observed after incubation for 17 days in the flask amended with MgO₂ and Fe₂O₃, but the number of compounds detected decreased (Figure 2D), which might be due to the full oxidation of some of these compounds. Because oxidized metabolites were less abundant in the control flask, partial chemical oxidation might have been at least partially responsible for the enhancement of palm oil dissolution and subsequent production of soluble compounds. This would corroborate the findings previously observed in other partial chemical oxidation studies.^{5,28,29,33,58,59} On the basis of our laboratory studies, partial chemical oxidation was shown to provide bioavailable (and biodegradable) oxidized compounds, and therefore, we performed a field scale experiment to test the feasibility of this approach in the environment.

The field experiment provided converging lines of evidence that supported the enhanced B100 compound dissolution and oxidation in the PCO-B experiment. This evidence included (i) the increase in acidity, (ii) the production of organic acids, (iii) the production of methane (as the environment was strongly anaerobic), and (iv) the decrease in redox (ORP) values. To evaluate the effects of partial chemical oxidation on biodiesel remediation, data from a past adjacent field release (100 L) with pure soybean biodiesel (B100) under MNA were used as a comparative control. In the PCO-B experiment, the production of both acetate (90 mg L⁻¹) and propionic acid (13.1 mg L⁻¹)

was observed after 3.4 months following the release (Figure 3A2,B2). In addition, increased acidity (from 25.1 to 420 mg of CaCO₃ L⁻¹) and methane production (from 0 to 4.9 mg L⁻¹) (Figure 3C2) were noted while ORP values decreased (from 259 to -137 mV). Although an increase in pH is commonly observed after oxidant delivery,^{15,16} in the PCO-B experiment the pH negligibly varied (from 5 to 4), and this was attributed to the slow release of H₂O₂ and to source-zone dilution (possibly because of rainfall infiltration as the experimental site was not covered with an impermeable layer). In the control experiment, organic acids and methane production were not observed at 3 months after B100 release (Figure 3A1,B1), and acidity values were considerably lower over the whole experimental time frame (20 months) (maximal concentration of 242.3 mg of CaCO₃ L⁻¹). These results provided evidence that partial chemical oxidation enhanced biodiesel FAME oxidation and dissolution to the groundwater.

Soil source-zone analyses conducted at the end of the monitoring period in both PCO-B (after 30.6 months) and MNA (after 99.2 months) experiments indicated a complete removal of biodiesel LNAPL. Results for oil and grease were below the detection limit for all samples in both experiments [<10 mg (kg of soil)⁻¹]. In the MNA experiment, the TOC concentration in the source zone [832.4 ± 207.3 mg (kg of soil)⁻¹] was similar to that in the background well [803 mg (kg of soil)⁻¹], while in PCO-B, the TOC concentration was lower in the source zone [630 ± 136.2 mg (kg of soil)⁻¹] than in the background well [936 mg (kg of soil)⁻¹], possibly because of the organic matter oxidation by peroxides. The more sensitive source-zone groundwater TOC analyses showed that TOC in the MNA groundwater (21 mg L⁻¹) was twice that in the PCO-B groundwater (10 mg L⁻¹) (Figure S6). Given the low acetate concentration in this time frame in the MNA experiment (0.6 mg L⁻¹), larger hydrocarbon compounds might have persisted in the groundwater and, thus, provide evidence that biodiesel has not been fully remediated even 8 years after the release. Comparatively, in the PCO-B experiment, the acetate concentration was even lower (0.15 mg L⁻¹) and methane concentrations (11.3 mg L⁻¹) were on the same order of magnitude as the TOC concentration (10 mg L⁻¹) (Figure S6). This is consistent with enhanced biodiesel FAME degradation in the PCO-B site compared to that in the MNA site.

The release of soluble and bioavailable compounds to the groundwater by partial chemical oxidation is likely to stimulate microbial growth, and thus, biodegradation could be used as a joint strategy to remove residual organic compounds. On the basis of qPCR data (Figure S5), total bacteria increased from 10⁶ to 10⁸ gene copies g⁻¹ after 3.4 months, reaching concentrations as high as 10¹⁴ gene copies g⁻¹ 12.4 months following the release. In contrast, the total concentration of bacteria in the control MNA experiment was considerably lower (10⁸ gene copies g⁻¹) 20 months following the release. Hence, the enhanced release of biodegradable oxidized compounds by partial chemical oxidation probably stimulated the microbial activity as reflected by the high total concentration of bacteria relative to that in the control experiment.

To gain insight into the microbial communities that evolve during the release of biodiesel oxidized compounds as well as to discern key players involved in B100 biodegradation, 16S rRNA gene sequencing was performed. The production of soluble oxidized biodiesel compounds promoted a beneficial response in microbial communities. Groundwater conditions were

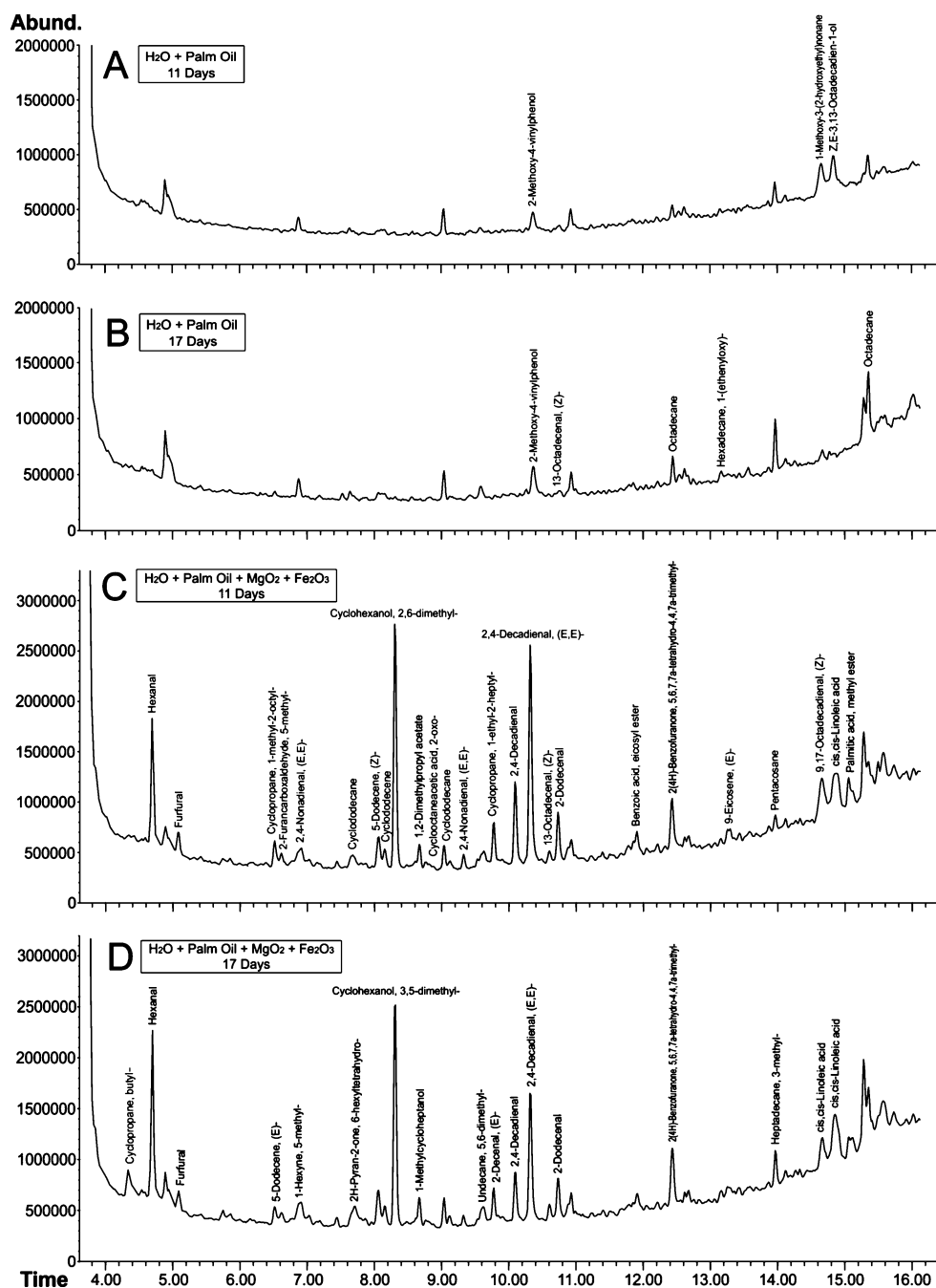


Figure 2. GC chromatograms of palm oil batch experiments (sets 3 and 6) after incubation for 11 and 17 days. Set 3 (control), distilled water and palm oil after (A) 11 and (B) 17 days. Set 6: distilled water, palm oil, MgO₂, and Fe₂O₃ after (C) 11 and (D) 17 days.

aerobic at the beginning of the experiment (1.4 months) as shown by the positive ORP values (241 mV) and supported by the predominance of aerobic and facultative genera (Figure 4A,B). Detailed information about the putative metabolism and respiration mode of all microbial genera detected in both PCO-B and MNA field experiments is available in Table S3. Anaerobic conditions that were likely established by the high biochemical oxygen demand exerted by biodiesel compounds⁴³ were observed 3.4 months following the release with a decrease in ORP (from 241 to -137 mV) and DO concentration (from 2.4 to 0.5 mg L⁻¹) and a concomitant production of methane (up to 4.9 mg L⁻¹) (Figure 3C2). Related shifts in microbial community structure from predominantly aerobic to anaerobic genera (Figure 4A,B) followed the geochemical trends. A

selection of microbial populations implicated in biodiesel oxidized compound (organic acids, aldehydes, and alcohols) biodegradation was observed (Figure 4A–D), and dominance shifted toward the putative anaerobic hydrocarbon degraders *Geobacter* and *Desulfosporosinus* between 3.4 and 6.4 months in SWS. These genera are known for their ability to oxidize a wide variety of organic compounds such as fatty acids, alcohols, sugars, and organic acids. *Geobacter* is a well-studied iron reducer typically associated with aromatic hydrocarbon degradation in acetate-rich environments,^{60–62} as was the case for the PCO-B experiment (acetate concentrations of ≤ 278.4 mg L⁻¹). *Desulfosporosinus* generally thrives with sulfate, thiosulfate, or sulfite as an electron acceptor^{63,64} to partially oxidize alcohols, sugars, and organic acids to acetate,⁶⁴ and its

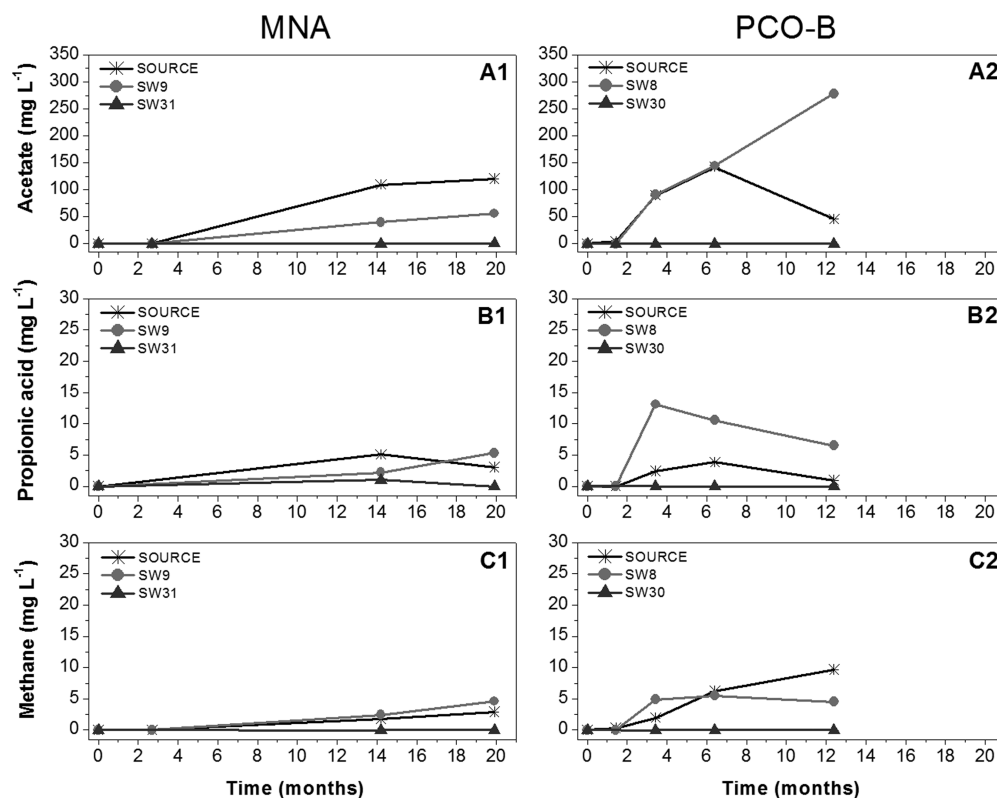


Figure 3. Geochemical footprint of B100 releases of the MNA and PCO-B plots. The figure shows acetate (A1 and A2), propionic acid (B1 and B2), and methane (C1 and C2) concentrations 2 m (MNA) and 3 m (PCO-B) bgs.

ability to use Fe^{3+} as an electron acceptor has also been demonstrated.^{64,65} A similar pattern was observed later for SW8 (from 6.4 to 13.4 months), possibly because it was installed 1.5 m down gradient of the SWS and the slow groundwater flow (6 m year⁻¹) might have delayed the migration of compounds to this sampling well. The predominance of *Geobacter* and *Desulfosporosinus* in both SWS and SW8 was chronologically coherent with the increase in Fe^{2+} concentration (from 27 to 229.5 mg L⁻¹), which is consistent with these organic compounds having been biodegraded under iron reducing conditions. Furthermore, *Pelotomaculum* and *Clostridium* detected in both SWS and SW8 may have also contributed to the overall biodegradation, because the former is associated with propionate oxidation and some members are obligate syntrophs,⁶⁶ while *Clostridium* is typically regarded as a primary fermenter, although some species have also been implicated in fatty acid and acetate oxidation.^{67–70} The metabolic features of the main bacterial genera found in the PCO-B experiment support their putative role as key players implicated in biodiesel oxidized compound degradation, and the metabolites commonly produced by these bacteria are acetate, hydrogen, and carbon dioxide,⁷⁰ depending on the substrates available. These genera have also been observed to cooperate with archaeal communities in syntrophic relations^{62,64,71,72} to exploit the minimal energetic yield commonly observed in strongly anaerobic environments.

Microbial communities benefit energetically from syntrophic relations with different partners by combining their metabolic capabilities to consume a substrate that cannot be independently catabolized,^{73,74} thus underscoring the important role played by syntrophic microbial interactions (e.g., between bacteria and archaea) for the complete removal of contami-

nants. The presence of methanogens coincided with the increased methane concentrations (up to 9.7 mg L⁻¹) observed 12.4 months after the release. In the PCO-B experiment, all archaeal communities detected in the groundwater are putatively capable of exploiting the hydrogenotrophic pathway (*Candidatus methanoregula*, *Methanomassiliicoccus*, *Methanospirillum*, and *Methanocella*)^{66,75,76} (Figure 4C,D). Although 16S rRNA gene (V3–V4 region of *rrs*) sequencing analyses provide phylogenetic information and cannot be used to reach conclusions about microbial functionality, the presence of acetogenic and acetoclastic bacteria along with hydrogenotrophic archaea is consistent with their cooperation in syntrophy to alleviate eventual thermodynamic constraints posed by metabolite (e.g., acetate and hydrogen) accumulation to favor the complete removal of contaminants.

The geochemical footprint of the MNA control experiment 20 months after the release had chemical conditions similar to those of the PCO-B experiment; thus, a 16S rRNA gene sequencing analysis was conducted at this time to gain insight into the microbial communities involved in B100 natural attenuation. Results revealed the presence of the bacterial genera *Erwinia*, *Desulfosporosinus*, and *Clostridium* in the source 20 months following the release (Figure S3). Although the *Erwinia* genus contains facultative anaerobes ecologically associated with plants⁷⁷ and has not yet been associated with biodiesel esters or long-chain fatty acid biodegradation, it can produce organic acids via fermentative pathways⁷⁸ that could justify its abundance at this point in time. The high relative abundance of *Erwinia*, *Desulfosporosinus*, and *Clostridium* coincided with the highest concentration of acetate (120.6 mg L⁻¹) (Figure 3A1) and Fe^{2+} (99.5 mg L⁻¹) after 20 months, which is consistent with the B100 compounds having been

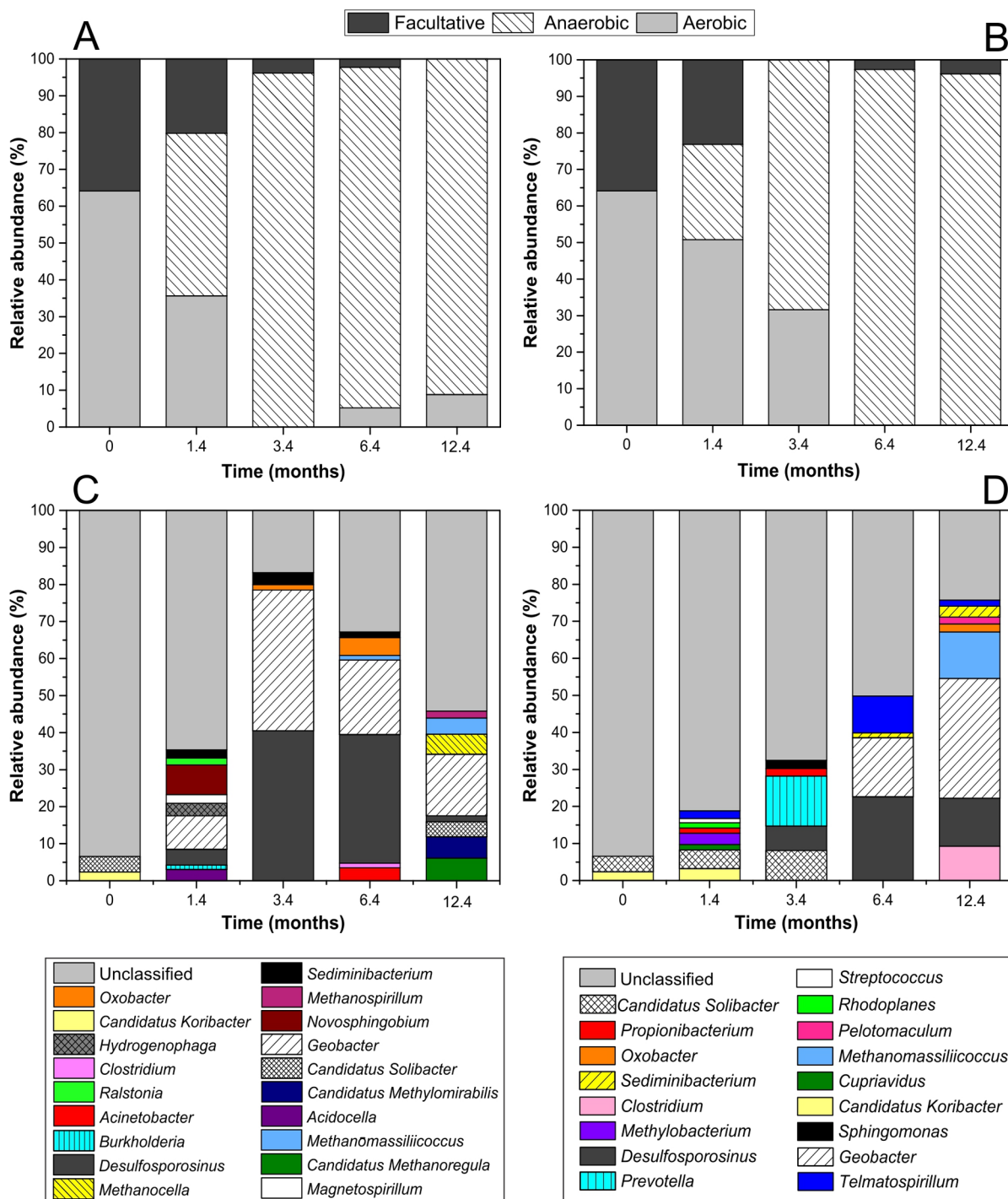


Figure 4. Temporal changes in the 16S rRNA microbial community relative abundance of the PCO-B experiment. Respiration mode of microbial community relative abundance in (A) SWS and (B) SW9 (without depicting unclassified genera). 16S rRNA relative abundance in microbial communities detected in (C) SWS and (D) SW8. Samples were collected at 3 m bgs. Charts depict microbial genera with a relative abundance of $\geq 1\%$.

biodegraded under fermentative and iron reducing conditions. Similar syntrophic relations may have also taken place in the control experiment after 20 months as reflected by the presence of the hydrogenotrophic archaeal genera *Methanomassiliicoccus* and *Methanocella* as they coincided with the highest methane concentration (4.6 mg L^{-1}) detected in the MNA experiment (Figure 3C1). Given that shifts in microbial populations coincided with the enhanced organic acids and methane production in both experiments and that geochemical and

microbial community profiles in the MNA experiment reached conditions similar to those in the PCO-B experiment only 20 months after the release, the PCO-B treatment appears to have enhanced the overall B100 remediation rate as compared to the rate of natural attenuation processes.

In summary, batch and field experiments demonstrated an enhanced dissolution and production of soluble oxidation compounds as well as the faster production of organic acids compared to the MNA control experiment. This difference was

attributed to the partial chemical oxidation of the biodiesel. Microbial activity inhibition was not observed, and the beneficial response of microbial populations implicated in biodiesel oxidized compound biodegradation was attributed to the release of bioavailable compounds that led to a shift in relative microbial abundance toward *Geobacter* and *Desulfosporosinus* genera, both of which might be key players involved in biodiesel oxidized compound anaerobic biodegradation. This is the first field experiment to demonstrate that partial chemical oxidation (with MgO_2 and Fe_2O_3 , AMD) coupled to biodegradation could be a feasible approach for the removal of poorly water-soluble compounds that behave as LNAPLs and prevent the long-term effects generally posed in source zones.

■ ASSOCIATED CONTENT

Supporting Information

The Supporting Information is available free of charge on the ACS Publications website at DOI: 10.1021/acs.est.6b03604.

Schematic view of the experimental area configuration (PCO-B and MNA control experiments), 16S rRNA relative abundance (percent) of microbial communities in groundwater samples from SWS and SW31 from the MNA experiment 20 months following the release, GC chromatograms of soybean oil batch experiments after incubation for 11 and 17 days, theoretical modified Fenton reactions with MgO_2 and Fe_2O_3 and organic compound termination reactions, concentration of total bacteria (qPCR of 16S rRNA gene) at the source zone of the PCO-B experiment, groundwater concentrations (milligrams per liter) of total organic carbon (TOC), acetate, and methane at the source zone of MNA and PCO-B experiments 99.2 and 30.6 months following the release, respectively, primer sequences used for qPCR and 16S rRNA gene sequencing, and metabolic characteristics of the archaeal and bacterial communities in groundwater samples from B100 releases of PCO-B and MNA experiments (PDF)

■ AUTHOR INFORMATION

Corresponding Author

*E-mail: henry.corseuil@ufsc.br. Phone: +55 48 37212130. Fax: +55 48 32346459.

ORCID

Helen S. C. Lazzarin: 0000-0001-6085-193X

Notes

The authors declare no competing financial interest.

■ ACKNOWLEDGMENTS

This research was primarily funded by Petróleo Brasileiro S/A-PETROBRAS. Additional funds were provided by the National Council for Scientific and Technological Development (CNPq) [special visiting researcher program (PVE) and scholarships]. We thank Sébastien Cecillon for his help with the GC/MS analysis and Dr. Sandrine Demanche for the Illumina Miseq sequencing.

■ REFERENCES

(1) *Technical and Regulatory Guidance for in Situ Chemical Oxidation of Contaminated Soil and Groundwater*; In Situ Chemical Oxidation Team, Interstate Technology and Regulatory Council: Washington, DC, 2005.

(2) Krembs, F. J.; Siegrist, R. L.; Crimi, M. L.; Furrer, R. F.; Petri, B. G. ISCO for Groundwater Remediation: Analysis of Field Applications and Performance. *Groundwater Monit. Rem.* **2010**, *30* (4), 42–53.

(3) Siegrist, R. L.; Crimi, M.; Simpkin, T. J. *In Situ Chemical Oxidation for Groundwater Remediation*; Springer Science & Business Media: New York, 2011; Vol. 3.

(4) Siegrist, R. L.; Crimi, M.; Brown, R. A. In Situ Chemical Oxidation: Technology Description and Status. In *In Situ Chemical Oxidation for Groundwater Remediation*; Siegrist, R. L., Crimi, M., Simpkin, T. J., Eds.; Springer Science & Business Media: New York, 2011; pp 1–32.

(5) Valderrama, C.; Alessandri, R.; Aunola, T.; Cortina, J. L.; Gamisans, X.; Tuhkanen, T. Oxidation by Fenton's reagent combined with biological treatment applied to a creosote-contaminated soil. *J. Hazard. Mater.* **2009**, *166* (2–3), 594–602.

(6) Sutton, N. B.; Kalisz, M.; Krupanek, J.; Marek, J.; Grotenhuis, T.; Smidt, H.; de Weert, J.; Rijnaarts, H. H. M.; van Gaans, P.; Keijzer, T. Geochemical and Microbiological Characteristics during in Situ Chemical Oxidation and in Situ Bioremediation at a Diesel Contaminated Site. *Environ. Sci. Technol.* **2014**, *48* (4), 2352–2360.

(7) Feng, Y.; Lu, K.; Mao, L.; Guo, X.; Gao, S.; Petersen, E. J. Degradation of 14C-labeled few layer graphene via Fenton reaction: Reaction rates, characterization of reaction products, and potential ecological effects. *Water Res.* **2015**, *84*, 49–57.

(8) Sutton, N. B.; Atashgahi, S.; Saccenti, E.; Grotenhuis, T.; Smidt, H.; Rijnaarts, H. H. M. Microbial Community Response of an Organohalide Respiring Enrichment Culture to Permanganate Oxidation. *PLoS One* **2015**, *10* (8), e0134615.

(9) Liang, C.; Lee, L.-L. In situ iron activated persulfate oxidative fluid sparging treatment of TCE contamination — A proof of concept study. *J. Contam. Hydrol.* **2008**, *100* (3–4), 91–100.

(10) Bianchi-Mosquera, G. C.; Allen-King, R. M.; Mackay, D. M. Enhanced Degradation of Dissolved Benzene and Toluene Using a Solid Oxygen-Releasing Compound. *Groundwater Monit. Rem.* **1994**, *14* (1), 120–128.

(11) Xie, G.; Barcelona, M. J. Sequential chemical oxidation and aerobic biodegradation of equivalent carbon number-based hydrocarbon fractions in jet fuel. *Environ. Sci. Technol.* **2003**, *37* (20), 4751–4760.

(12) Schmidtke, T.; White, D.; Woolard, C. Oxygen release kinetics from solid phase oxygen in Arctic Alaska. *J. Hazard. Mater.* **1999**, *64* (2), 157–165.

(13) Vol'nov, I. I.; Latysheva, E. I. Thermal stability of magnesium peroxide. *Bull. Acad. Sci. USSR, Div. Chem. Sci.* **1970**, *19* (1), 11–15.

(14) Elprince, A. M.; Mohamed, W. H. Catalytic Decomposition Kinetics of Aqueous Hydrogen Peroxide and Solid Magnesium Peroxide By Birnessite. *Soil Sci. Soc. Am. J.* **1992**, *56* (6), 1784.

(15) Waite, A. J.; Bonner, J. S.; Autenrieth, R. Kinetics and Stoichiometry of Oxygen Release from Solid Peroxides. *Environ. Eng. Sci.* **1999**, *16* (3), 187–199.

(16) Cassidy, D. P.; Irvine, R. L. Use of calcium peroxide to provide oxygen for contaminant biodegradation in a saturated soil. *J. Hazard. Mater.* **1999**, *69* (1), 25–39.

(17) Liu, G.; Porterfield, D. M. Oxygen enrichment with magnesium peroxide for minimizing hypoxic stress of flooded corn. *J. Plant Nutr. Soil Sci.* **2014**, *177* (5), 733–740.

(18) Goi, A.; Viisimaa, M.; Trapido, M.; Munter, R. Polychlorinated biphenyls-containing electrical insulating oil contaminated soil treatment with calcium and magnesium peroxides. *Chemosphere* **2011**, *82* (8), 1196–1201.

(19) Magnesium Peroxide. Solvay America, Inc., 2013.

(20) Walling, C. Fenton's reagent revisited. *Acc. Chem. Res.* **1975**, *8* (4), 125–131.

(21) Bergendahl, J. A.; Thies, T. P. Fenton's oxidation of MTBE with zero-valent iron. *Water Res.* **2004**, *38* (2), 327–334.

(22) Petri, B. G.; Watts, R. J.; Teel, A. L.; Huling, S. G.; Brown, R. A. Fundamentals of ISCO Using Hydrogen Peroxide. In *In Situ Chemical Oxidation for Groundwater Remediation*; Siegrist, R. L., Crimi, M.,

Simpkin, T. J., Eds.; Springer Science & Business Media: New York, 2011; pp 33–88.

(23) Flores, R. G.; Andersen, S. L. F.; Maia, L. K. K.; José, H. J.; Moreira, R. d. F. P. M. Recovery of iron oxides from acid mine drainage and their application as adsorbent or catalyst. *J. Environ. Manage.* **2012**, *111*, 53–60.

(24) Sutton, N. B.; Grotenhuis, J. T. C.; Langenhoff, A. A. M.; Rijnaarts, H. H. M. Efforts to improve coupled in situ chemical oxidation with bioremediation: a review of optimization strategies. *J. Soils Sediments* **2011**, *11* (1), 129–140.

(25) Liang, C.; Lee, I.-L.; Hsu, I.-Y.; Liang, C.-P.; Lin, Y.-L. Persulfate oxidation of trichloroethylene with and without iron activation in porous media. *Chemosphere* **2008**, *70* (3), 426–435.

(26) Cassidy, D.; Northup, A.; Hampton, D. The effect of three chemical oxidants on subsequent biodegradation of 2,4-dinitrotoluene (DNT) in batch slurry reactors. *J. Chem. Technol. Biotechnol.* **2009**, *84* (6), 820–826.

(27) Mundle, K.; Reynolds, D. A.; West, M. R.; Kueper, B. H. Concentration Rebound Following In Situ Chemical Oxidation in Fractured Clay. *Groundwater* **2007**, *45* (6), 692–702.

(28) Kao, C. M.; Wu, M. J. Enhanced TCDD degradation by Fenton's reagent preoxidation. *J. Hazard. Mater.* **2000**, *74* (3), 197–211.

(29) Kaludjerski, M.; Gurol, M. D. Assessment of enhancement in biodegradation of dichlorodiethyl ether (DCDE) by pre-oxidation. *Water Res.* **2004**, *38* (6), 1595–1603.

(30) Kulik, N.; Goi, A.; Trapido, M.; Tuhkanen, T. Degradation of polycyclic aromatic hydrocarbons by combined chemical pre-oxidation and bioremediation in creosote contaminated soil. *J. Environ. Manage.* **2006**, *78* (4), 382–391.

(31) Ndjou'ou, A.-C.; Bou-Nasr, J.; Cassidy, D. Effect of Fenton Reagent Dose on Coexisting Chemical and Microbial Oxidation in Soil. *Environ. Sci. Technol.* **2006**, *40* (8), 2778–2783.

(32) Gong, X.-B. Remediation of weathered petroleum oil-contaminated soil using a combination of biostimulation and modified Fenton oxidation. *Int. Biodeterior. Biodegrad.* **2012**, *70*, 89–95.

(33) Nam, K.; Rodriguez, W.; Kukor, J. J. Enhanced degradation of polycyclic aromatic hydrocarbons by biodegradation combined with a modified Fenton reaction. *Chemosphere* **2001**, *45* (1), 11–20.

(34) National Council of Energy Policy. Brazil. Law 13.263, March, 23rd, 2016. Altera a Lei n° 13.033, de 24 de setembro de 2014, para Dispor sobre os percentuais de adição de biodiesel ao óleo diesel comercializado no território nacional (Altera Law 13.033, September, 2014, and establishes the percentage required for the addition of biodiesel to diesel oil sold to final consumers in Brazil) (http://www.planalto.gov.br/ccivil_03/_Ato2015-2018/2016/Lei/L13263.htm).

(35) *Biofuels: Release Prevention, Environmental Behavior, and Remediation*; Biofuels Team, Interstate Technology and Regulatory Council: Washington, DC, 2011.

(36) Fang, H. L.; McCormick, R. L. Spectroscopic Study of Biodiesel Degradation Pathways. *SAE Tech. Pap. Ser.* **2006**, DOI: 10.4271/2006-01-3300.

(37) Karavalakis, G.; Stournas, S.; Karonis, D. Evaluation of the oxidation stability of diesel/biodiesel blends. *Fuel* **2010**, *89* (9), 2483–2489.

(38) Østerstrøm, F. F.; Anderson, J. E.; Mueller, S. A.; Collings, T.; Ball, J. C.; Wallington, T. J. Oxidation Stability of Rapeseed Biodiesel/Petroleum Diesel Blends. *Energy Fuels* **2016**, *30* (1), 344–351.

(39) Akhlaghi, S.; Hedenqvist, M. S.; Conde Braña, M. T.; Bellander, M.; Gedde, U. W. Deterioration of acrylonitrile butadiene rubber in rapeseed biodiesel. *Polym. Degrad. Stab.* **2015**, *111*, 211–222.

(40) Saxena, P.; Hildemann, L. M. Water-soluble organics in atmospheric particles: A critical review of the literature and application of the thermodynamics to identify candidate compounds. *J. Atmos. Chem.* **1996**, *24* (1), 57–109.

(41) Bruice, P. Y. *Organic Chemistry*, 4th ed.; 2004; Vol. 1.

(42) Andersen, S. L. F.; Flores, R. G.; Madeira, V. S.; José, H. J.; Moreira, R. F. P. M. Synthesis and Characterization of Acicular Iron Oxide Particles Obtained from Acid Mine Drainage and Their

Catalytic Properties in Toluene Oxidation. *Ind. Eng. Chem. Res.* **2012**, *51* (2), 767–774.

(43) Corseuil, H. X.; Monier, A. L.; Gomes, A. P. N.; Chiaranda, H. S.; do Rosario, M.; Alvarez, P. J. J. Biodegradation of Soybean and Castor Oil Biodiesel: Implications on the Natural Attenuation of Monoaromatic Hydrocarbons in Groundwater. *Groundwater Monit. Rem.* **2011**, *31* (3), 111–118.

(44) Lage, I. d. C. Avaliação de metodologias para determinação da permeabilidade em meios porosos: a área experimental da Fazenda Ressecada, SC (Evaluation of methods to determine permeability in porous media: the experimental site of Fazenda Ressecada, SC). Ph.D. Dissertation, Universidade Federal do Rio de Janeiro, Rio de Janeiro, 2005.

(45) Franson, M. A. H. *Standard methods for the examination of water and wastewater*, 18th ed.; American Public Health Association, American Water Works Association and Water Environment Federation: Washington, DC, 1994.

(46) Lehman, R. M.; Colwell, F. S.; Bala, G. A. Attached and unattached microbial communities in a simulated basalt aquifer under fracture- and porous-flow conditions. *Appl. Environ. Microbiol.* **2001**, *67* (6), 2799–2809.

(47) Harvey, R. W.; Smith, R. L.; George, L. Effect of organic contamination upon microbial distributions and heterotrophic uptake in a Cape Cod, Mass., aquifer. *Appl. Environ. Microbiol.* **1984**, *48* (6), 1197–1202.

(48) 16S Metagenomic Sequencing Library Preparation. Illumina, Inc. Techonology.

(49) FASTX-Toolkit (http://hannonlab.cshl.edu/fastx_toolkit/) (accessed May 31, 2016).

(50) Masella, A. P.; Bartram, A. K.; Truszkowski, J. M.; Brown, D. G.; Neufeld, J. D. PANDAseq: paired-end assembler for illumina sequences. *BMC Bioinf.* **2012**, *13*, 31.

(51) Caporaso, J. G.; Kuczynski, J.; Stombaugh, J.; Bittinger, K.; Bushman, F. D.; Costello, E. K.; Fierer, N.; Peña, A. G.; Goodrich, J. K.; Gordon, J. I.; et al. QIIME allows analysis of high-throughput community sequencing data. *Nat. Methods* **2010**, *7* (5), 335–336.

(52) Edgar, R. C. Search and clustering orders of magnitude faster than BLAST. *Bioinformatics* **2010**, *26* (19), 2460–2461.

(53) Northup, A.; Cassidy, D. Calcium peroxide (CaO₂) for use in modified Fenton chemistry. *J. Hazard. Mater.* **2008**, *152* (3), 1164–1170.

(54) Liu, H.; Bruton, T. A.; Doyle, F. M.; Sedlak, D. L. In situ chemical oxidation of contaminated groundwater by persulfate: decomposition by Fe(III)- and Mn(IV)-containing oxides and aquifer materials. *Environ. Sci. Technol.* **2014**, *48* (17), 10330–10336.

(55) Rivas, F. J. Polycyclic aromatic hydrocarbons sorbed on soils: A short review of chemical oxidation based treatments. *J. Hazard. Mater.* **2006**, *138* (2), 234–251.

(56) Lundstedt, S.; Persson, Y.; Öberg, L. Transformation of PAHs during ethanol-Fenton treatment of an aged gasworks' soil. *Chemosphere* **2006**, *65* (8), 1288–1294.

(57) Silva, P. T. de S. E.; Silva, V. L. da; Neto, B. de B.; Simonnot, M.-O. Phenanthrene and pyrene oxidation in contaminated soils using Fenton's reagent. *J. Hazard. Mater.* **2009**, *161* (2–3), 967–973.

(58) Martens, D. A.; Frankenberger, W. T. J. Enhanced degradation of polycyclic aromatic hydrocarbons in soil treated with an advanced oxidative process — Fenton's Reagent. *Soil Sediment Contam.* **1995**, *4* (2), 175–190.

(59) Lee, B. D.; Hosomi, M. A hybrid fenton oxidation-microbial treatment for soil highly contaminated with benz(a)anthracene. *Chemosphere* **2001**, *43* (8), 1127–1132.

(60) Lovley, D. R. Microbial Fe(III) reduction in subsurface environments. *FEMS Microbiol. Rev.* **1997**, *20* (3–4), 305–313.

(61) Lovley, D. R. Bug juice: harvesting electricity with microorganisms. *Nat. Rev. Microbiol.* **2006**, *4* (7), 497–508.

(62) Ramos, D. T.; da Silva, M. L. B.; Nossa, C. W.; Alvarez, P. J. J.; Corseuil, H. X. Assessment of microbial communities associated with fermentative-methanogenic biodegradation of aromatic hydrocarbons

in groundwater contaminated with a biodiesel blend (B20). *Biodegradation* **2014**, *25* (5), 681–691.

(63) Robertson, W. J.; Bowman, J. P.; Franzmann, P. D.; Mee, B. J. *Desulfosporosinus meridiei* sp. nov., a spore-forming sulfate-reducing bacterium isolated from gasoline-contaminated groundwater. *Int. J. Syst. Evol. Microbiol.* **2001**, *51* (1), 133–140.

(64) Sánchez-Andrea, I.; Stams, A. J. M.; Hedrich, S.; Nancucneo, I.; Johnson, D. B. *Desulfosporosinus acididurans* sp. nov.: an acidophilic sulfate-reducing bacterium isolated from acidic sediments. *Extremophiles* **2015**, *19* (1), 39–47.

(65) Bertel, D.; Peck, J.; Quick, T. J.; Senko, J. M. Iron transformations induced by an acid-tolerant *Desulfosporosinus* species. *Appl. Environ. Microbiol.* **2012**, *78* (1), 81–88.

(66) Imachi, H.; Sakai, S.; Sekiguchi, Y.; Hanada, S.; Kamagata, Y.; Ohashi, A.; Harada, H. *Methanolinea tarda* gen. nov., sp. nov., a methane-producing archaeon isolated from a methanogenic digester sludge. *Int. J. Syst. Evol. Microbiol.* **2008**, *58* (1), 294–301.

(67) Schink, B. Energetics of syntrophic cooperation in methanogenic degradation. *Microbiol. Mol. Biol. Rev. MMBR* **1997**, *61* (2), 262–280.

(68) Singleton, D. R.; Powell, S. N.; Sangaiah, R.; Gold, A.; Ball, L. M.; Aitken, M. D. Stable-Isotope Probing of Bacteria Capable of Degrading Salicylate, Naphthalene, or Phenanthrene in a Bioreactor Treating Contaminated Soil. *Appl. Environ. Microbiol.* **2005**, *71* (3), 1202–1209.

(69) Chauhan, A.; Ogram, A. Phylogeny of Acetate-Utilizing Microorganisms in Soils along a Nutrient Gradient in the Florida Everglades. *Appl. Environ. Microbiol.* **2006**, *72* (10), 6837–6840.

(70) Sieber, J. R.; McInerney, M. J.; Gunsalus, R. P. Genomic insights into syntrophy: the paradigm for anaerobic metabolic cooperation. *Annu. Rev. Microbiol.* **2012**, *66*, 429–452.

(71) Grabowski, A.; Blanchet, D.; Jeanthon, C. Characterization of long-chain fatty-acid-degrading syntrophic associations from a biodegraded oil reservoir. *Res. Microbiol.* **2005**, *156* (7), 814–821.

(72) Kato, S.; Hashimoto, K.; Watanabe, K. Methanogenesis facilitated by electric syntrophy via (semi)conductive iron-oxide minerals. *Environ. Microbiol.* **2012**, *14* (7), 1646–1654.

(73) Stams, A. J. M.; Plugge, C. M. Electron transfer in syntrophic communities of anaerobic bacteria and archaea. *Nat. Rev. Microbiol.* **2009**, *7* (8), 568–577.

(74) Schink, P. B.; Stams, A. J. M. Syntrophism Among Prokaryotes. In *The Prokaryotes*; Rosenberg, E., DeLong, E. F., Lory, S., Stackebrandt, E., Thompson, F., Eds.; Springer: Berlin, 2013; pp 471–493.

(75) Bräuer, S. L.; Cadillo-Quiroz, H.; Yashiro, E.; Yavitt, J. B.; Zinder, S. H. Isolation of a novel acidiphilic methanogen from an acidic peat bog. *Nature* **2006**, *442* (7099), 192–194.

(76) Dridi, B.; Fardeau, M.-L.; Ollivier, B.; Raoult, D.; Drancourt, M. *Methanomassiliicoccus luminyensis* gen. nov., sp. nov., a methanogenic archaeon isolated from human faeces. *Int. J. Syst. Evol. Microbiol.* **2012**, *62* (Part8), 1902–1907.

(77) Paulin, J. P. *Erwinia amylovora*: General characteristics, biochemistry and serology. In *Fire blight: The disease and its causative agent, Erwinia amylovora*; Vanneste, J. L., Ed.; CABI: Wallingford, CT, 2000; pp 87–115.

(78) Sutton, D. D.; Starr, M. P. Anaerobic dissimilation of glucose by *Erwinia amylovora*. *J. Bacteriol.* **1959**, *78* (3), 427–431.